Dynamic Pressure Loads Associated with Twin Supersonic Plume Resonance

John M. Seiner,* James C. Manning,† and Michael K. Ponton*
NASA Langley Research Center, Hampton, Virginia

The phenomenon of twin supersonic plume resonance is defined and studied as it pertains to high-level dynamic loads in the internozzle region of aircraft like the F-15 and B-1B. Using a 1/40th-scale-model twin jet nacelle with powered choked nozzles, it is found that intense internozzle dynamic pressures are associated with the phased coupling of each plume's large-scale structure. This condition is most prevalent when each plume's large-scale structure has constituent elements composed of the B-type helical instabilities. The coupling of each plume's large-scale structure forces each plume to flap spatially in a preferred direction. Suppression of these dynamic loads was accomplished by simple geometric modifications to only one plume's nozzle. These modifications disrupt the natural selection of the B-type mode and thereby decouple the plumes.

Nomenclature

D	= jet exit diameter
D_j	= fully expanded jet plume diameter, Eq. (4)
f_s	= plume resonance frequency
L	= average plume shock cell spacing, Eq. (5)
M_c	= convection Mach number large scale structure
M_d	= nozzle design Mach number
M_j	= fully expanded plume Mach number
St	= Strouhal number, Eq. (3)
V_c	= convection velocity of large-scale structure
V_j	= fully expanded jet plume velocity
γ	= ratio of specific heats
λ	= acoustic wavelength

Introduction

THIS paper is concerned with dynamic pressure fluctuations that exist in the internozzle region of those aircraft with twin-engine centerline spacings of two nozzle diameters or less. Aircraft such as the F-15 and B-1B use a very closely spaced engine configuration, and each is known to have suffered fatigue failures to engine nozzle outer flaps in the internozzle region. On the F-15 airplane, the fatigue failure of the engine nozzle flaps led the USAF to remove them from active duty aircraft. As a result, it is believed that there is a loss of installed performance (5–7 drag counts). Since the physical mechanism for this failure was never uncovered in prior investigations, concerns exist for potential fatigue failures to the maneuvering flaps associated with rectangular geometry nozzles.

Berndt's[1] dynamic pressure measurements on the B-1A aircraft suggest that this damage could be related to the existence of a high-energy narrow-band process in the internozzle region. In this paper, it is proposed that the physical origin of this narrow-band process is actually related to the phenomenon of supersonic plume resonance (i.e., jet screech, see Ref. 2), which for the twin-plume problem could be expected to produce enhanced growth rates for the governing shear-layer instabilities. This, in turn, would lead to a significant increase in energy scattered upon interaction with a shock wave and, thus, to exceptionally high dynamic pressures for the internozzle region.

In order to investigate this possibility for the F-15 and B-1B aircraft, a 1/40th-scale-model twin-jet nacelle with powered choked axisymmetric nozzles was constructed. Both the full-scale F-15 and B-1B aircraft have the same engine centerline spacing in their twin-jet nacelles. Both internozzle dynamic pressures and optical phase-averaged schlieren records of the plume flowfield were acquired for this study. The results have shown that a significant increase in the dynamic internozzle pressure can occur when each plume's governing instability is associated with helical spatial structure of the B-type plume resonance mode. Under these circumstances, the twin-plume instability wave structures were found to be effectively coupled and have much larger growth rates. Methods for suppression of this twin supersonic plume resonance phenomenon were also investigated and are reported in this paper.

Apparatus and Instrumentation

The 1/40th-scale-model twin-jet nacelle with powered twin-choked axisymmetric nozzles is shown in Fig. 1. This nacelle is constructed with a nozzle-to-nozzle centerline spacing of 1.9 jet exhaust diameters. The model is powered with dry, unheated air and fed from a common reservoir. The model's choked tubes are 45.72 cm long with a diameter of 1.57 cm. Each tube is equipped with a static pressure port near the exit plane to account for the large axial tube pressure gradient and thereby enable calculation of the fully expanded plume Mach number M_j. These static ports are located 0.12 cm from each tube's exit plane azimuthally along the opposite outer side of each nozzle.

A B&K 4136 pressure microphone was placed in the internozzle region at the exit plane to measure airborne dynamic pressures associated with the plume resonance phenomenon. In addition to this sensor, two others were placed in the exit plane along a common line joining the internozzle sensor but on opposite sides of each nozzle as illustrated in Fig. 1. These two outer sensors were used to determine the governing spatial mode of instability through transfer and coherence measurements, with the internozzle sensor as a reference. All other autospectra and amplitude data reported were measured by the internozzle sensor.

Received April 8, 1986; presented as Paper 86-1539 at the AIAA/ASME/SAE/ASEE 22nd Joint Propulsion Conference, Huntsville, AL, June 16–18, 1986; revision received Feb. 10, 1988.

*Aerospace Technologist. Member AIAA.

†Aerospace Technologist.

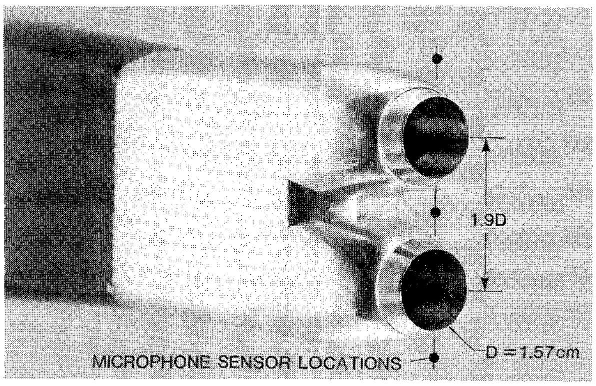

Fig. 1 F-15 model empennage (1/40th scale).

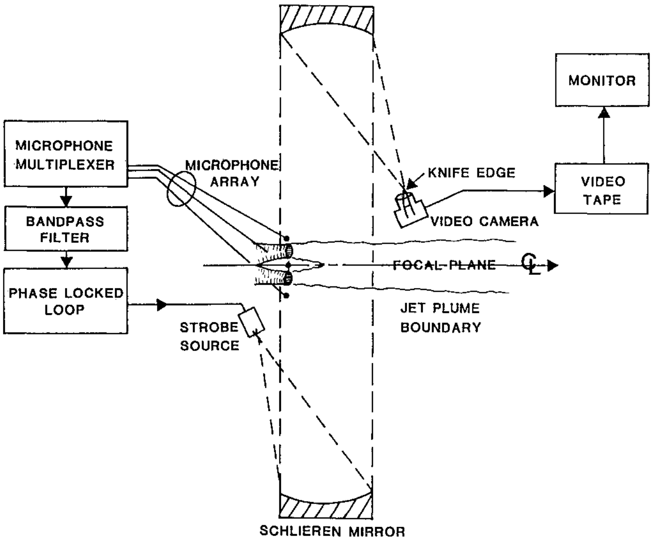

Fig. 2 Phase-averaged schlieren experimental system.

The internozzle sensor also served as a reference to obtain phase-averaged schlieren 70-mm photographic and video records. These optical records were also used to assist in identification of the spatial mode of instability associated with any large-amplitude pressure fluctuation. Figure 2 schematically illustrates the experimental arrangement used to obtain phase-averaged schlieren video records. The internozzle sensor's signal was buffered, bandpass-filtered 100 Hz around a resonance peak f_s, and fed to a phase-locked loop. The output from this circuit was a pulse train whose phase and frequency were locked to the bandpassed pressure fluctuations in the internozzle region. The phase relationship between these fluctuations and the output strobe signal was parametrically varied from 0 to 2π. The actual strobe frequency was selected as a submultiple of the bandpassed center frequency (typically 1/4 to 1/5 of f_s), since in most cases, frequencies of interest exceeded the lamp driver's frequency response.

The strobe source was a xenon flashlamp with a 1.5-mm spark gap. Optical pulse durations were in the order of a few μ/s. Two 30.5-cm-diam parabolic mirrors with 183-cm focal lengths were used to collimate the light beam. The knife edge was oriented vertically so that density gradients in the flow were along the axis of the plume. A lens was used with the video camera and 70-mm camera to provide a focused image of the plume on the vidicon and/or film plane.

Experimental Results

Autospectrum

A characteristic frequency spectrum of the pressure fluctuations in the internozzle region is shown in Fig. 3. This spectral

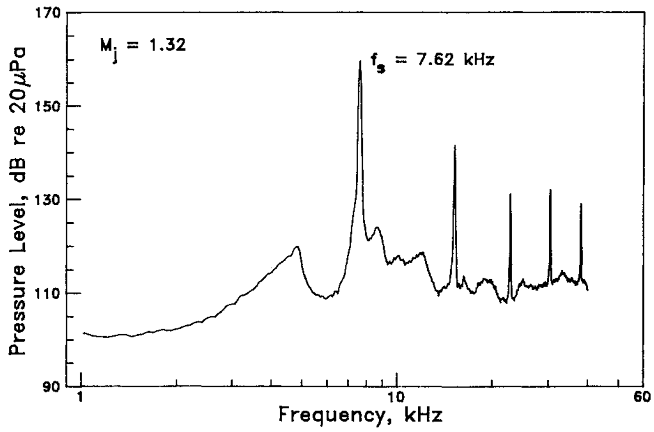

Fig. 3 Typical narrow-band spectra of internozzle pressure fluctuations.

record refers to operation of the twin-jet model in the underexpanded mode at a pressure ratio corresponding to a nozzle with a fully expanded Mach number M_j of 1.32. This spectral data shows the existence of a high-amplitude discrete process with harmonic tones through the fifth order. This discrete process clearly dominates the pressure fluctuations at this sensor location. The fundamental frequency f_s of 7.62 kHz, as is shown later, is the plume resonance frequency of concern in this paper. The spatial properties of the waves associated with this frequency can be examined through transfer and coherence measurements with the other two dynamic sensors.

Coherence and Phase of Modal Structure

The two additional dynamic sensors are located along the outer nozzle periphery at the exit plane as indicated in Fig. 1. Coherence and transfer function measurements were made between these two sensors as well as the one placed in the internozzle region. Figures 4a and 4b, respectively, show the degree of coherence between the right-hand nozzle sensor, the innernozzle sensor, and the left-hand nozzle sensor. As shown, in the spectral region surrounding f_s, all wave motion is perfectly correlated. Corresponding transfer function measurements in Figs. 5a and 5b further show that the waves along the outer plume periphery are anticorrelated with those between the plumes at and around the frequency f_s. The waves along the outer plume peripheries are in phase, as shown in Fig. 5b. These results clearly indicate that the governing instability wave at $M_j = 1.32$ is associated with an antisymmetric spatial structure. Optical visualization of these results can be demonstrated by centering the bandpass filters of Fig. 2 around the frequency f_s and recording on film or video the wave motion corresponding to various phases of the resonant cycle. This permits an in-depth examination of the flowfield structure associated with this particular fluctuating pressure.

Phase-Averaged Optical Records

The flowfield structure associated with the tone f_s in Fig. 3 is shown in the typical phase-averaged schlieren records of Figs. 6a and 6b. These records differ in phase by 180 deg relative to an incoming peak pressure wave in the internozzle region. These records are obtained by photographically averaging 32 phase-locked strobes to the flashlamp. As a result, unrelated turbulent structures are averaged to a constant contrast, and it is then possible, as shown, to identify the spatial mode of instability to be associated with the resonance peak f_s.

In the example of Fig. 6, the spatial mode of instability is helical and, as is shown later, it can be identified as a B-mode type. Each plume, however, contains two equal but oppositely rotating B-type helicies so that each plume is flapping in a preferred plane. When the instability wave structures of the two plumes are coupled together, the plane of flapping, imposed by boundary conditions, lies normal to the photographic plane in

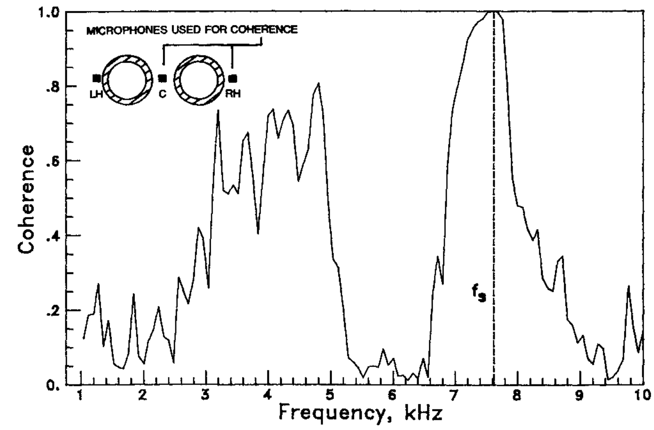

a) Right-hand relative to center sensor

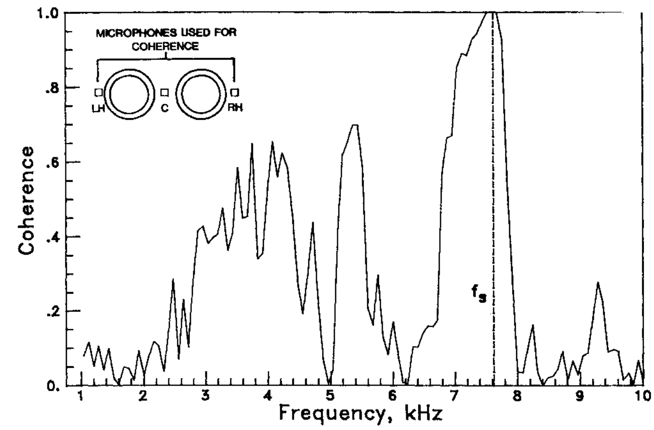

b) Right-hand relative to left-hand sensor

Fig. 4 Coherence of wave structure across twin-nozzle plane.

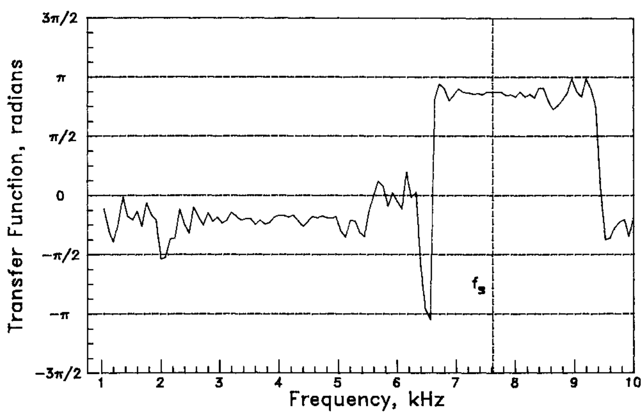

a) Right-hand relative to center sensor

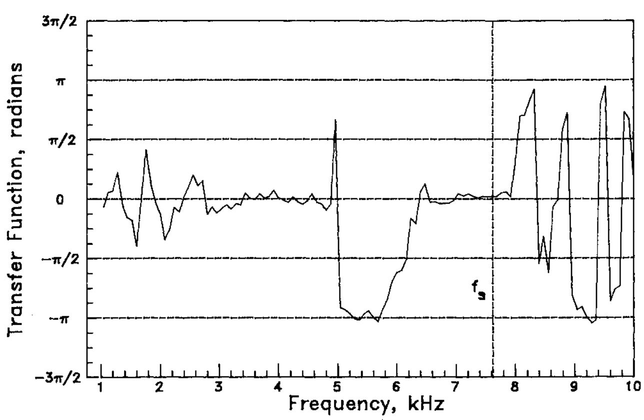

b) Right-hand relative to left-hand sensor

Fig. 5 Phase of wave structure across twin-nozzle plane.

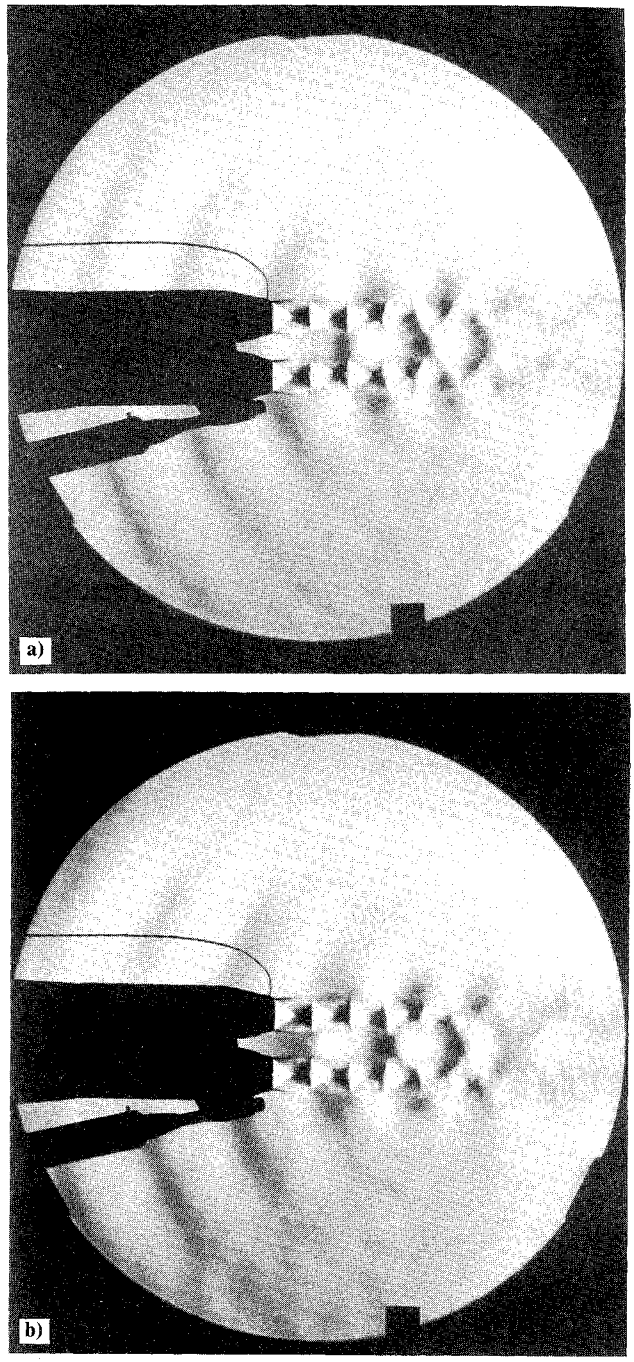

Fig. 6 Phase-averaged schlieren record of twin plumes at $M_j = 1.32$: a) relative phase $\phi = 0$, and b) relative phase $\phi = \pi$.

Fig. 6. Within this plane, the plumes are flapping antisymmetrically. When the two plumes are not coupled, the orientation of each plume's flapping plane is arbitrary.

The optical records of Fig. 6, however, clearly show that the twin-plume structures are coupled. Comparison of the shock cell structure between Figs. 6a and 6b shows a reversal in orientation that corresponds to the phase-locked firing sequence used to obtain these records. Associated phase-averaged video records additionally show intense pressure waves emanating from a region near the fourth shock cell that propagates upstream. Strong wave motion can be observed in the region between and along the outside periphery of both plumes. The intense acoustic waves along the outer plume periphery, here visible as alternating light and dark bands, also provide evidence that the two plume flowfields are coupled together. Even though each wave front is generated by a different plume, both arrive at each nozzle's exit simultaneously, as shown in Fig. 6a. The optical records of Figs. 6a and 6b provide the visual evidence for the coherence and transfer measurements discussed earlier.

An important property associated with the flapping mode of a coupled twin-plume configuration is the directional behavior of the emitted pressure waves. Minimum pressure amplitudes are expected for pressure waves radiated at angles normal to the flapping plane. That is, we would expect the acoustic waves along the outer plume periphery to be less intense when viewed at an angle 90 deg to the view in either Fig. 6a or 6b. To examine the directional behavior of the pressure waves, the phase-averaged schlieren record of Fig. 7 was obtained by rotating the twin-jet model 90 deg. It shows that the intensity of the propagating pressure waves have fallen below the resolution capabilities of the schlieren system. Thus, we see that the directional pattern associated with the resonance peak f_s consists of high-pressure peaks along the axis containing both nozzles and minimum levels in directions normal to this axis. This pressure pattern agrees with the circumferential distribution of dynamic surface pressure recorded by Berndt[1] around the periphery of his engine nozzle in model transonic tunnel studies.

The peak pressure levels along the line joining each nozzle is of special interest for fatigue-related concerns, particularly in the internozzle region, where fatigue failures of engine flaps have already occurred. It is, therefore, important to determine the nozzle pressure range of interest where plume coupling can be expected based on the current model. This can be done by examining the spectral amplitude and frequency dependence with the fully expanded plume Mach number M_j.

Resonant Modes of Single Choked Tube Jet

The resonance modes of a single choked tube jet were measured as part of this study. This was accomplished by simply blocking the flow path of the tube's nozzle. The purpose in doing this was to enable determination of any special features associated with the coupled twin-plume resonance phenomenon. Fundamental resonance frequencies f_s, like that shown in Fig. 3, were recorded over an extensive range of the parameter M_j.

The results are shown in Fig. 8. The data are presented in terms of acoustic wavelength normalized by the jet tube exit diameter. The dynamic sensor used to acquire this data is the one placed in the internozzle region at the tube nozzle's exit. As shown, many resonant modes exist, often appearing simultaneously with this type of nozzle. The various modes have been labeled according to established convention,[3] except for the E mode, which does not appear to have been measured by previous investigators. Based on the full set of optical records obtained in this study, the spatial structure for several of these modes is identified in Fig. 8. The amplitude behavior of these various modes is shown in Fig. 9, although only those modes are shown that achieve a maximum pressure level over 130 dB. From Fig. 9 it is observed that only one mode basically

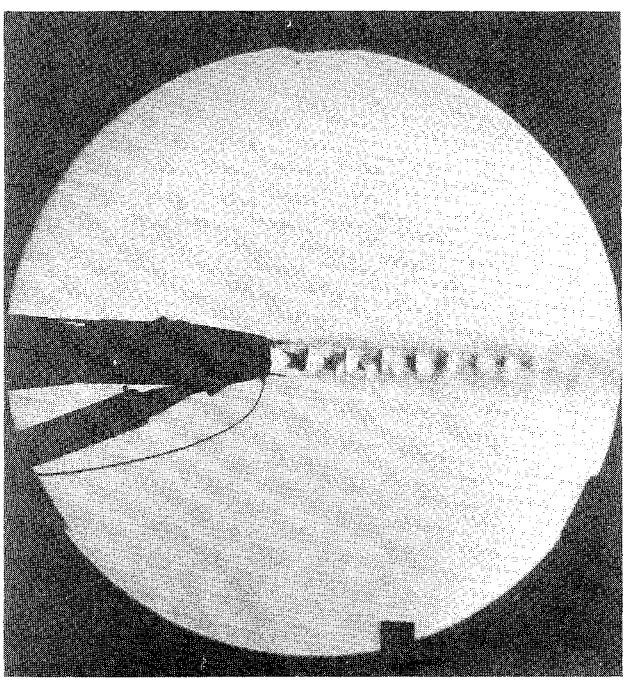

Fig. 7 Phase-averaged schlieren record of twin plumes at $M_j = 1.32$ with view rotated 90 deg.

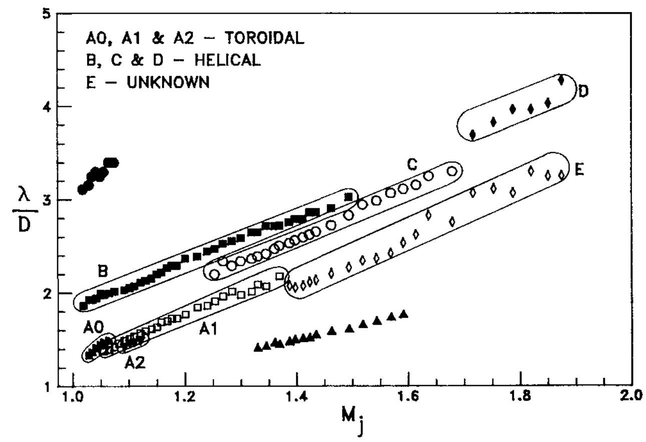

Fig. 8 Modal structure associated with single choked tube nozzle.

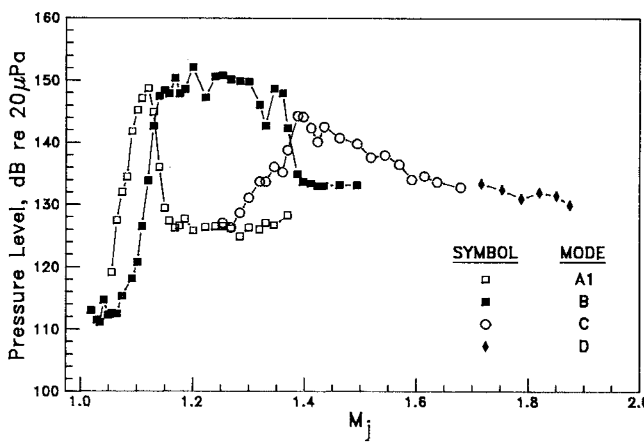

Fig. 9 Modal amplitude dependence with M_j for single choked tube nozzle.

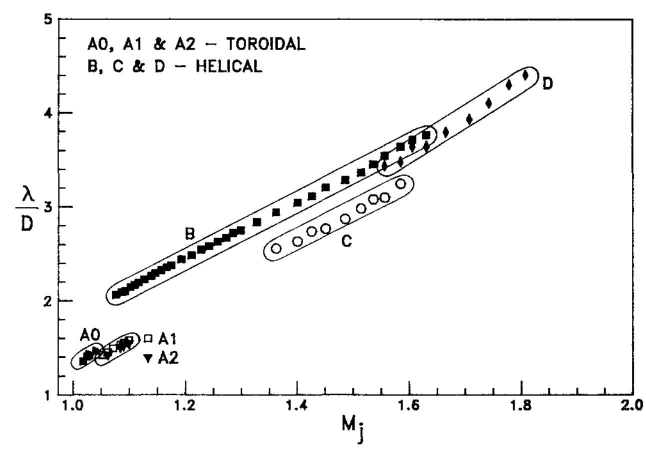

Fig. 10 Modal structure associated with twin choked tube nozzles.

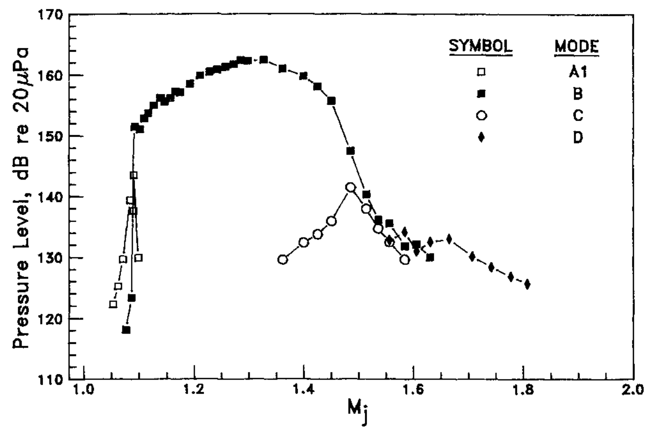

Fig. 11 Modal amplitude dependence with M_j for twin choked tube nozzles.

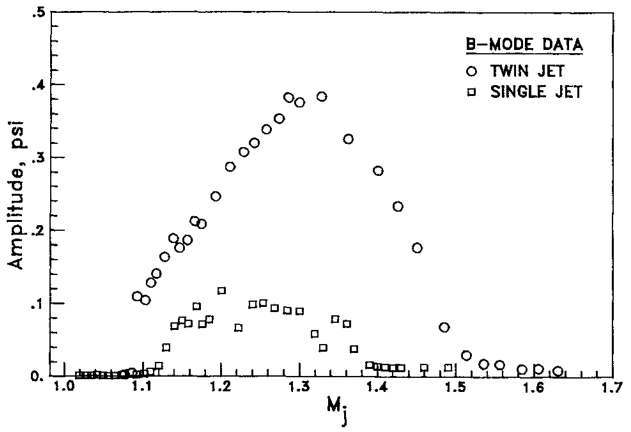

Fig. 12 Comparison of B-type helical mode amplitude behavior between single and twin jets.

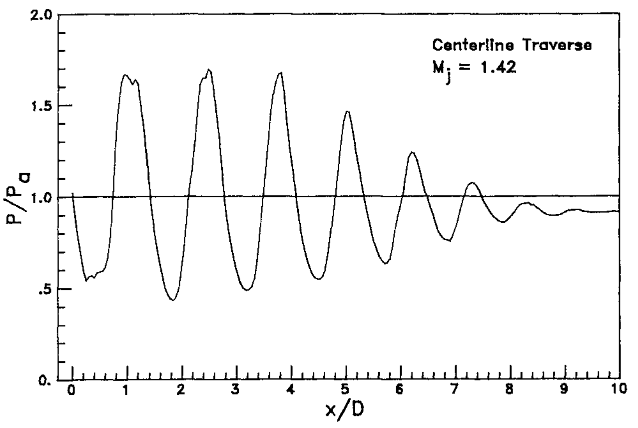

Fig. 13 Centerline static pressure data.

dominates the plume for any given M_j and that toroidal spatial structure only dominates a very small region at low values of M_j. Phase-averaged schlieren results illustrating the nature of toroidal structure are reported in Ref. 3.

Resonant Modes of Twin Choked Tube Jet

Using the same dynamic sensor, fundamental resonance frequencies for the twin-jet configuration were acquired over a similar range of the parameter M_j. These results are presented in Fig. 10, again in terms of normalized acoustic wavelength λ/D. Comparison of these results with the single choked tube data of Fig. 8 show that the twin jet has fewer modal structures than the single jet. It can also be observed that acoustic wavelengths become relatively longer than those of the single jet, with increasing values of M_j. This is presumably due to shock wave stretching caused by mutual interaction of the twin plumes.

The associated amplitude data for the modes of Fig. 10 are presented in Fig. 11. From this data, it is evident that dominant pressure levels can be associated with the B-type helical mode structure. The single-jet results of Fig. 9 also have shown that this is the dominant mode. However, the twin-jet results show that this type of modal structure is more prevalent over a much wider range of plume Mach numbers.

The maximum amplitude levels achieved by the twin-jet configuration are considerably greater than could be expected from simply doubling the pressure levels associated with the single jet. The difference is readily apparent in Fig. 12, where only the amplitudes of the B-type helical mode are presented on a linear scale for the single and twin jet. From this figure, it is apparent that in the range $1.15 \le M_j \le 1.5$ the amplitudes associated with the twin jet exceed the single jet amplitudes by a factor of greater than 2. Thus, over this range of plume Mach numbers, the twin-jet plumes appear to have coupled instability wave modes. While it is not yet possible to predict the near-field amplitude behavior shown in Fig. 12 for the B-type helical mode, its frequency can be predicted adequately.

Prediction of Resonant Frequency

The model for the physical mechanism of single-jet resonance was originally developed by Powell.[2] His model was based on a linear array of monopole radiators, whose phase was dependent on a turbulent eddy's convection time between the monopole radiators. The monopole radiators were located equally spaced at shock termination points derivable from Pack's[4] linearized analysis. To make the model work, Powell assumed that certain turbulent eddies were shed from the nozzle lip by feedback from upstream propagating waves and that these eddies would have a spatial coherence of many shock cell wavelengths.

Powell's frequency formula derivable from this model can be written for the fundamental resonance tone as

$$f_s = V_c/L(1 + M_c) \tag{1}$$

where L, V_c, and M_c are the shock wavelength, convection velocity, and Mach number of a turbulent eddy, respectively. Equation (1) can also be predicted from the quasilinear instability wave modal analysis method,[5] where V_c and M_c represent the convective parameters of axisymmetric or helical modal structures that interact with the shock wave field. Using the crossed laser beam experiments of Harper-Bourne and Fisher,[6] the convection velocity of the large-scale structure is estimated as

$$V_c = 0.7V_j \tag{2}$$

Thus, the resonant frequency f_s of Eq. (1) can be written in terms of a nondimensional Strouhal number as

$$St = \frac{f_s D_j}{V_j} = \frac{0.7(D_j/D)}{L/D(1 + M_c)} \tag{3}$$

where from Tam and Tanna[7] the ratio of the fully expanded plume diameter D_j to the jet exit diameter is given by

$$\frac{D_j}{D} = \left\{\frac{[1 + (\gamma - 1)/2]\, M_j^2}{[1 + (\gamma - 1)/2]\, M_d^2}\right\}^{(\gamma+1)/4(\gamma-1)} \left(\frac{M_d}{M_j}\right)^{1/2} \tag{4}$$

The shock spacing of Eq. (3) is derived from Pack's linearized analysis or from the more accurate numerical[8,9] or analytical[10] methods. However, these methods severely underestimate the

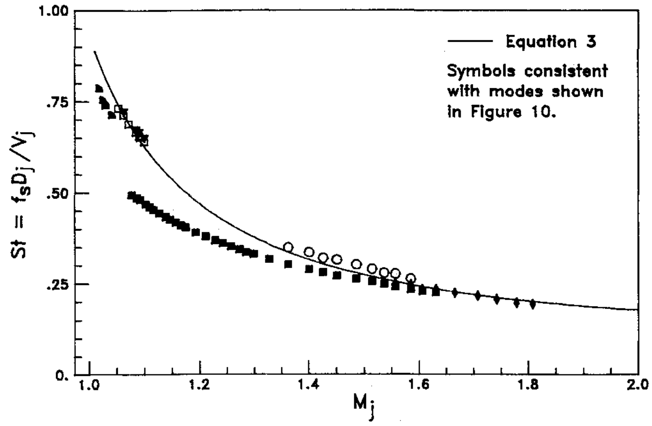

Fig. 14 Prediction of the twin-jet resonant frequency.

shock wavelength found in a twin-plume model whose wave field is coupled.

In this study, the shock wavelength was determined empirically through experimental measurement of the plume static pressure. The method for doing this has been fully described in Ref. 9, where an average shock cell spacing is determined from static pressure measurements like those of Fig. 13. In Fig. 13, P is the plume static pressure and P_a is the surrounding ambient pressure. Determination of an average shock wavelength L over a range of M_j values produced the following empirical correlation for use in Eq. (3):

$$L/D = 2.06M_j - 1.6 \tag{5}$$

Comparison of Eq. (5) with results from Ref. 9 on the single choked nozzle shows that the twin-plume configuration of this study has shock wavelengths between 10 and 15% longer than the single jet.

In Fig. 14, comparison is made between the frequency data of Fig. 10 for the twin-jet model and that predicted by Eq. (3). As can be observed, the frequency of the resonant modes can be adequately predicted over a wide range of M_j. However, as can be noted, the theory only predicts a monomodal structure for a given M_j value. Thus, the theory tends to deviate substantially from the measured St values of the B-type helical mode at values of M_j less than 1.2.

Load Reduction by Plume Resonance Suppression

Thus far we have shown that the most prevalent spatial mode of instability is the jet flapping mode, with the B-type helical instability as the constituent element. When these modes are coupled between the twin plumes, large dynamic pressures are measured in the internozzle region. These values are beyond what could be justified by simply doubling the radiated power. These high dynamic levels attributed to twin-plume coupling represent a possible mechanism for the internozzle fatigue failure on the F-15 and B-1B aircraft.

Several passive methods of suppression were investigated. Figures 15a and 15b show the results achieved using two of the concepts investigated to reduce the internozzle pressure levels. The first method uses a small tab-like device mounted at the nozzle exit. The projected area for this device into the flow is on the order of 0.023 cm^2. The second method uses a small notch at the nozzle exit. The area of the notch is also on the order of 0.023 cm^2. The azimuthal location for either method appears arbitrary. These methods only involve minor geometric alteration to one nozzle of the twin configuration.

The open symbols in Fig. 15 refer to the unsuppressed B-type helical mode amplitude data of the twin jet. The solid symbols represent the result after a suppression concept is applied. The dashed line near 0.16 psi [i.e., 155 dB Sound Pressure Level (SPL)] represents a reference level above which sonic fatigue

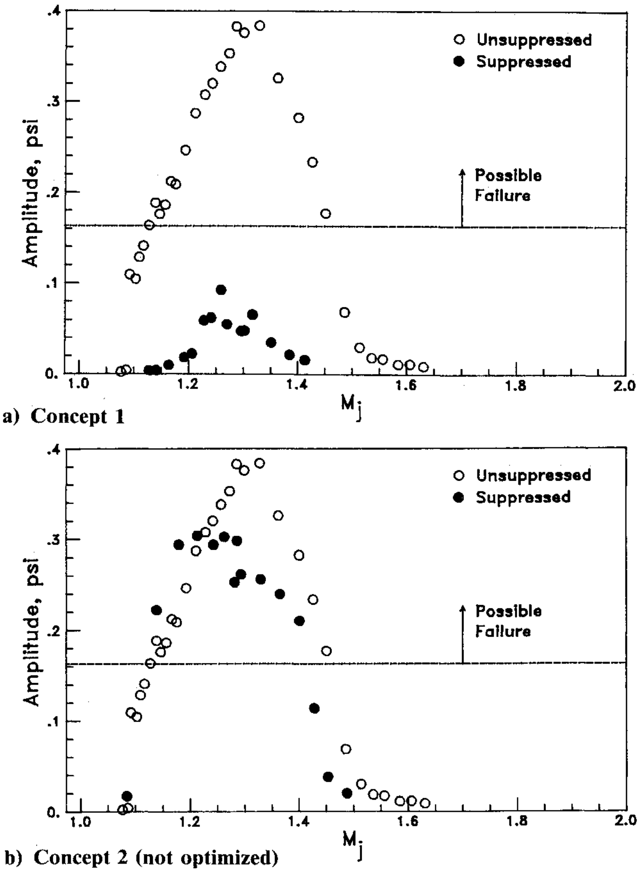

Fig. 15 Magnitude of dynamic pressure loads for B-type helical mode with and without suppression.

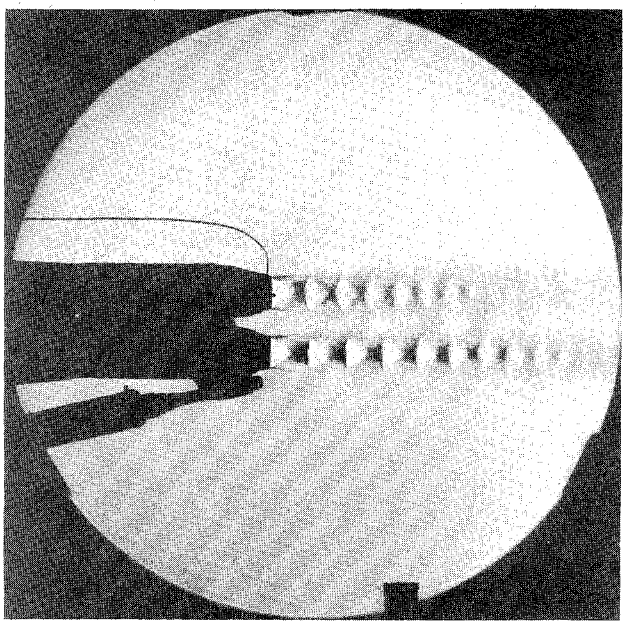

Fig. 16 Phase-averaged schlieren record showing twin-plume resonancel suppression at $M_j = 1.32$.

and crack growth problems usually can be expected.[11] Figure 15 shows that concept 1 provides an adequate suppression method, whereas concept 2 does not provide sufficient load reduction. In either case, neither of these concepts involves significant loss of either nozzle's thrust, but instead, each concept alters the preferred wave structure between each plume so that no coupling is possible.

The phase-averaged schlieren record, Fig. 16, shows visual evidence of the result of applying suppression concept 1. This method only affects the upper plume in Fig. 16, where it can be observed that the wave structure between each plume is no longer equal, the plumes are uncoupled, and the intense inner and outer pressure waves have been practically eliminated. Comparison of the suppressed twin plume with those shown in Fig. 6 shows that suppression of the B-type helical mode in one plume drastically diminishes the plume spread rate of both plumes.

Conclusions

In this paper, the mechanism of twin supersonic plume resonance is defined and its properties studied as a possible mechanism for engine nozzle flap fatigue failure on the F-15 and B-1B aircraft. Using a 1/40th-scale-model twin-jet nacelle with powered choked axisymmetric nozzles, it is found that excessive internozzle dynamic pressures can be associated with the phased coupling of each plume's jet-flapping mode. This condition is most prevalent when each plume's jet-flapping mode has constituent elements composed of the B-type helical instability. This instability is distinguished from others in that its axial wavelength is a near-integer multiple of the shock wave spacing. When selected, this mode produces the fastest natural spread rate for the supersonic jet plume. In the present twin axisymmetric study, the range of influence of the B-type instability is found to cover fully expanded Mach numbers ranging from 1.15 to 1.50. The directional behavior of this mechanism is found to agree well with the circumferential surface dynamic sensor measurements of Berndt.[1]

Amplitude levels recorded when the plumes were coupled exceeded levels generally associated with fatigue failure for aircraft metallic-type structures. By passively detuning one of the two nozzle plumes from selecting the B-type helical instability, suppression of these dynamic levels to acceptable standards was achieved. Suppression concepts investigated in this study involved only minor geometric changes to the nozzle, where the loss of thrust would be expected to be minimal. Not investigated, and representing a study of its own, was the minimum nozzle separation distance required to prevent the coupling of each plume's jet-flapping mode.

Future studies of the twin supersonic plume resonance phenomenon as defined in this paper involve the use of model-scale convergent-divergent axisymmetric and two-dimensional twin-powered engine nacelles. The nozzle design shapes would closely follow the philosophy used in full-scale engines. Both static and full-scale test of an F-15 aircraft have been planned, since the effect of forward flight and temperature both modify the selection of a supersonic plume's governing instability.

References

[1]Berndt, D. E., "Dynamic Pressure Fluctuations in the Internozzle Region of a Twin-Jet Nacelle," Society of Automotive Engineers, Warrendale, PA, TP-841540, Oct. 1984.

[2]Powell, A., "On the Mechanism of Choked Jet Noise," *Proceedings of the Physical Society,* London, Sec. B, Vol. 66, 1953, pp. 1039–1056.

[3]Seiner, J. M., "Advances in High Speed Jet Aeroacoustics," AIAA Paper 84-2275, Oct. 1984.

[4]Pack, D. C., "A Note on Prandtl's Formula for the Wavelength of a Supersonic Jet," *Quarterly Journal of Mechanics and Applied Mathematics,* Vol. 3, Pt. 2, June 1950, pp. 173–181.

[5]Tam, C. K. W., Seiner, J. M., and Yu, J. C., "On the Relationship Between Broadband Shock Associated Noise and Screech Tones," AIAA Paper 84-2276, Oct. 1984.

[6]Harper-Bourne, M. and Fisher, M. J., *The Noise from Shock Waves in Supersonic Jets,"* AGARD-CP-131, 1973.

[7]Tam, C. K. W. and Tanna, H. K., "Shock Associated Noise of Supersonic Jets from Convergent-Divergent Nozzles," *Journal of Sound Vibrations,* Vol. 81, No. 3, April 1982, pp. 337–358.

[8]Dash, S. M., Wolf, D. E., and Seiner, J. M., "Analysis of Turbulent Underexpanded Jets, Part I: Parabolized Navier-Stokes Model, SCIPVIS," *AIAA Journal,* Vol. 23, April 1985, pp. 505–514.

[9]Seiner, J. M., Dash, S. M., and Wolf, D. E., "Analysis of Turbulent Underexpanded Jets, Part II: Shock Noise Features Using SCIPVIS," *AIAA Journal,* Vol. 23, May 1985, pp. 669–677.

[10]Tam, C. K. W., Jackson, J. A., and Seiner, J. M., "A Multiple-Scales Model of the Shock-Cell Structure of Imperfectly Expanded Supersonic Jets," *Journal of Fluid Mechanics,* Vol. 153, April 1985, pp. 123–149.

[11]Guinn, W. A., Balena, F. J., and Soovere, J., "Sonic Environment of Aircraft Structure Immersed in a Supersonic and Jet Flow Stream," NASA CR-144996, 1976.